Dynamic Properties of a Hydraulic Servo Actuator Flexibly Connected to a Load Mass Excited by Cyclic Force

Ryszard Dindorf (dindorf@tu.kielce.pl)
Politechnika Swietokrzyska https://orcid.org/0000-0002-2242-3288
Piotr Wos
Politechnika Swietokrzyska

Original Article

Keywords: Hydraulic servo actuator, Hydraulic boom manipulator, Flexible connections, Cyclic impact force, Position controller, Adaptive identification

Posted Date: June 9th, 2020

DOI: https://doi.org/10.21203/rs.3.rs-34070/v1

Dynamic Properties of a Hydraulic Servo Actuator Flexibly Connected to a Load Mass Excited by Cyclic Force

Ryszard Dindorf [1,*] and Piotr Wos [1]

[1] Faculty of Mechatronics and Mechanical Engineering, Department of Manufacturing Engineering and Metrology, Kielce University of Technology, al. Tysiaclecia Panstwa Polskiego 7, 25-314 Kielce, Poland

* Correspondence: dindorf@tu.kielce.pl

Abstract

The study deals with the dynamic properties of a hydraulic servo actuator (HSA) with flexible mounting connections. This problem is considered in two cases: firstly, in the flexible (or non-rigid) mounting connection of the barrel and piston rod of a hydraulic actuator, and secondly, in the vibration isolation of a hydraulic actuator loaded with cyclic force. The difficult and complex dynamic problem of an HSA flexibly connected to a load mass excited by the impact force generated by a rock breaker was primarily analysed. The solution of a new design of the 3-DoF hydraulic boom manipulator used to move a medium-sized hydraulic rock breaker was presented. The HSA is rigidly mounted to the mother boom, and the piston rod is flexibly connected to the inner boom via a spring-damping device (SDD), which, in this case, serves as a vibration isolator. Simulation tests based on the HSA mathematical model enabled comparison of the dynamic responses of the hydraulic actuator rigidly connected and flexibly connected via an SDD to a load mass excited by the constant and impact force generated by a rock breaker. The experimental studies on the test stand focused on HSA adaptive positioning control. The main task was to adapt the adaptive position controller to the identified HSA loaded with excitation force (impact force). The simulation and experimental tests carried out are important for assessing dynamic properties and designing the position controller of an HSA subjected to cyclic impact forces. The presented results are also important for the development of guidelines for the safe operation of various large-scale heavy hydraulic machines under vibration loads.

Keywords: Hydraulic servo actuator, Hydraulic boom manipulator, Flexible connections, Cyclic impact force, Position controller, Adaptive identification

1. Introduction

Dynamic properties and precision of control of hydraulic servo actuators (HSAs) depend on the rigidity of the mounting of its components: actuators (barrels, piston rods), control elements (valves), load mass and equipment. The connections between hydraulic and mechanical elements in hydraulic drives are not always rigid, although it is usually assumed that these connections are always rigid. This approach even applies to vehicles on rough roads, heavy vehicles, aircraft, construction equipment, road vehicles, road-making machines, heavy-duty machines, agricultural machinery, mining machinery, machines in the steel industry, lifting equipment, transportation equipment as well as in heavy manipulators and robots. In such machines and hydraulic devices, load mass and external forces constantly change. At the same time, clearances in moving joints must be taken into account. Such operating conditions lead to the occurrence of vibrations and elastic deformations of the structural and connection elements of hydraulic devices. The vibrations are then transferred

to the hydraulic drive and control elements. The problem of the impact of both non-rigid or flexibility mounting of the hydraulic system design on its dynamic properties is taken into account extremely sporadically. A dynamic analysis of HSAs usually assumes that the load mass is rigidly connected to the piston rod of an actuator. Although this is the correct assumption for most industrial applications, there are some cases in which a non-rigid connection of the load mass should be considered. A non-rigid mounting of a hydraulic actuator barrel is sometimes also considered.

The dynamic properties of an HSA change dramatically if part of the moving mass is connected more or less flexibly to the piston rod, and/or if the actuator stands on a vibrating base. Such a situation frequently arises in hydraulically actuated machines, e.g. in rolling mills where the hydraulic actuator is completely integrated into the mill stand [1]. Ref. [2] presents the use of hydraulic actuators in four basic versions, taking into account their non-rigid mounting. The research paper was reviewed for non-rigid or flexible connection of hydraulic actuators. Ref. [3] presents a hydraulic control system with one degree of freedom with a flexible base and load contact. A single-acting hydraulic actuator that was connected to a non-rigid base and mass load was considered. The base of the actuator is not connected to a rigid ground, but to a flexible and moving base. This is the case with mobile work equipment in which a hydraulic actuator is connected to the machine frame, and the machine frame rides on flexible wheels. The piston rod-end is also connected to the mass load through a non-rigid tool mechanism. The interaction between the actuator and the mass load is modelled as an inertia, spring and damper system. In Ref. [4], the various dynamic performances of the linear model of a hydraulic actuator with elastically mounted mass, when the mass is inside or outside the feedback loop, was analysed. It has been established that the stiffness of the hydraulic actuator significantly affects the dynamic properties of the hydraulic drive. In Ref. [5], the influence of the impacts of various factors on the properties of the stiffness of hydraulic actuators was studied, including oil volume modulus, the air content of hydraulic oil, axial deformation of the piston rod, expansion of the barrel volume, expansion of the volume of metal pipes and flexible hoses and deformation of the seal. Ref. [6] presents spring-damper systems that were equivalent to the dynamic model of the hydraulic actuators. This actuator to lift a boom of a truck delivering concrete was used. In Ref. [7], dynamic stability tests of the actuator were carried out, determining the conditions of loss of its stability. Vibration models of hydraulic cylinders are usually adopted as beam models [8, 9], in which the analysis of vibration damping in beams modelling a barrel and a piston rod is performed. In Ref. [10], a method for the vibration analysis of a hydraulic pump was proposed. The dynamic responses of a hydraulic plunger pump are obtained through numerical simulation. In Ref. [11], a novel passive hydraulically interconnected suspension system is proposed to achieve an improved ride-handling compromise of mining vehicles. A lumped-mass vehicle model involved with a mechanical-hydraulic coupled system was developed by applying the free-body diagram method. Robots for heavy loads and/or wide operating ranges with flexible links have become a popular research object for control engineers, owing to their sophisticated properties [12]. The approach of an active damping control for multi-link flexible robots uses the spring-damper element, which is a passive energy dissipative device [13]. Hydraulic actuators fail as a result of physical damage or deterioration of their seals. Physical damage to the hydraulic actuator is usually caused by an external source, such as vibrations excited by a rock breaker. Actuator damage can take the form of a bent piston rod or dented barrel, both of which could prevent a full piston stroke. Physical damage can also occur in the actuator mounting parts. Since the hydraulic actuator is a single point of failure (SPOF), its reliability is very important in hydraulic actuation systems. The failure rate is expressed in

component failures per unit of time [14]. Ref. [15] presents a comprehensive assessment of the reliability of an aircraft's hydraulic power supply and control system. Military Standards (MIL-STAD) require compliance with good practices regarding the operation and maintenance of hydraulic systems and components [16]. For safety reasons, hydraulic components should be mounted in such a way that they are resistant to loosening due to excitation vibration [17].

In operating hydraulic drives, excessive vibrations are a common problem. These are not due to hydraulic reasons, but usually to mechanical reasons resulting from excited vibrations. When designing hydraulic drives, mechanical vibrations are not identified at all. The mechanical connections and device constructions are treated as rigid, and external payloads as constant. This means that mechanical vibrations are not taken into account either in the movement of the hydraulic actuators or during the operation of the control elements.

2. Formulating the research problem

Mechanical vibrations contribute to the operational and maintenance trouble of hydraulic components and systems. The designer of the hydraulic devices and systems should anticipate the potential problem associated with long-term mechanical vibration, and not just use easy and short-term solutions. This study considered the intentional introduction of a springy connection with damping as a vibration isolator. The application of spring-damping devices (SDD) reduces the transmission of vibrations from the excitation source to the elements of an HSA. In the case of an HSA loaded with vibration or impact forces, the use of an SDD is justified.

The study is related to the design of a hydraulic boom manipulator for a jaw crusher for the needs of a cement plant. Limestone is a rock block that should be crushed for further processing. The crusher breaks large rocks into smaller ones that are carried to the mill. Shredded rocks after milling in a mill and separating are calcined into quicklime. In jaw crushers, rock particles are crushed between a fixed and a moving plate (jaw). Jaw crushers easily crush rock of any material and size. For crushing, different jaws are used, with smooth adjustment of the grip angle with a special screw. Blake crushers are commonly used as primary crushers in the mineral industry. The size of the feed opening is referred to as the gape. The opening at the discharge end of the jaws is referred to as the set. The size of a jaw crusher is usually described by the gape and the width expressed as gape×width. In Blake jaw crushers, the largest rock particle size that can be crushed is equal to 0.9 gapes. The largest rocks particle size is generally ascertained by the blast pattern in the pit or the size of shovels and dump-cars used to transport the rocks from the mines. It is helpful to choose the size of the scalping screen that is placed on the rock conveyor in front of the crusher. . In the work of jaw crushers, there are frequent cases in which the rock conveyor and feed gape are blocked by too large rock particles. In this case, these large rock sizes must be crushed by a hand hammer by a worker in hazardous conditions. This causes downtime for the jaw crusher and reduces their productivity. Therefore, a hydraulic manipulator with a hydraulic rock breaker was designed to crush too large rocks located on the conveyor or in the feed gape. Figure 1 shows a diagram of a jaw crusher with a rock conveyor to which a hydraulic boom manipulator will be attached. The result of the study is to be an assessment of the design of an HSA controlled hydraulic manipulator with high load mass and cyclic exciting forces. Attempts are also being made to select an HSA control algorithm that would compensate for variable mass load and provide high precision positioning of the hydraulic boom. The designed hydraulic manipulator is used to move a medium-sized hydraulic rock breaker (up to 300 kg). Such a hydraulic rock

breaker is mounted on a telescopic boom, which is extended over a length of 1.2 m using an extension hydraulic actuator.

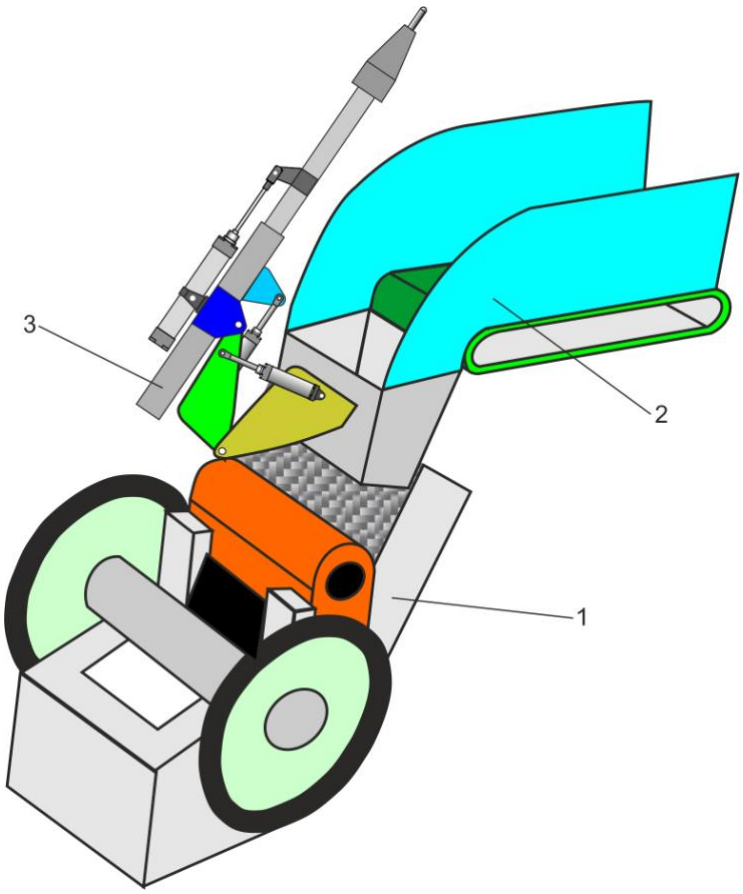

Figure 1. Schematic diagram of a rock crusher: 1 – Blake jaw crusher, 2 – rock conveyor, 3 – hydraulic boom manipulator

Figure 2 shows a schematic diagram of the solution for mounting a hydraulic actuator on a hydraulic boom manipulator.

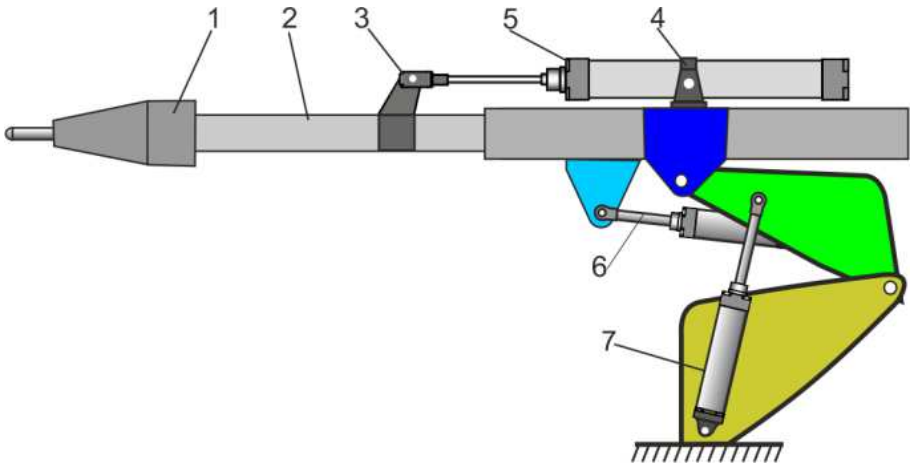

Figure 2. Design of a hydraulic boom manipulator: 1 – hydraulic rock breaker, 2 – telescopic boom, 3 – clevis bracket, 4 – center trunnion, 5 – inner boom actuator, 6 – rotation actuator, 7 – lift actuator

The hydraulic manipulator has three degrees of freedom (3-DoF), and its workspace includes the rock conveyor and feed gape. The kinematic structure of the hydraulic manipulator consists of an RRP serial kinematic chain with two rotary R joints and one prismatic P joint. The telescopic boom as a prismatic joint is the main element of the hydraulic manipulator. The double telescopic boom consists of the mother boom and the internal boom. The mother boom is lifted and rotated by a lifting actuator and a rotary actuator. The inner boom is extended and retracted by the boom actuator. The hydraulic manipulator was designed for a carrier weight of 2.5-3.5 t for which a rock breaker (SC25 Montabert) was selected. The parameters of this rock breaker are as follows: weight 225 kg, operating pressure (max) 120 bar, flow rate range 25-50 L/min, frequency 1,3100 bpm, tool diameter 55mm.

The study will be carried out mainly to determine the dynamic properties of an HSA when the actuator is rigidly mounted to the mother boom and the piston rod is flexibly connected to the inner boom via a spring-damping device (SDD) as a vibration isolator. The issue was analyzed when the inner boom is loaded with an external mass excited by impact force coming from the rock breaker. SDD is a spring device with viscoelastic damping elements. A spring with viscous damping devices enables effective damping of vibrations at high dynamic loads, such as a hydraulic rock breaker. Figure 3 shows the connection of the hydraulic actuator to the internal telescopic boom through an SDD.

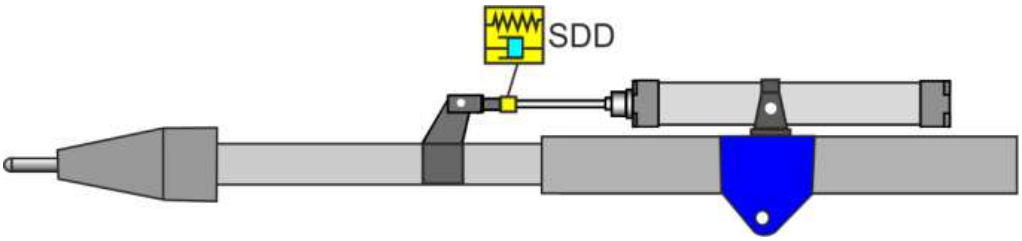

Figure 3. Hydraulic actuator connection to the internal telescopic boom through an SDD

3. Simulation model of HSA

A hydraulic servo actuator (HSA) was used, which consists of an asymmetric hydraulic actuator and a 4/3 (4-way, 3-position) proportional directional control valve with electrical position feedback and integrated electronics OBE (On-Board Electronics) [18]. The integrated electronics compare the specified command value to the actual position value of the main valve control spool. In the event of a control deviation, the respective control solenoid is controlled. A 3D model and view of such an HSA are shown in Figure 4. Placing a proportional directional control valve with a position controller directly on the hydraulic actuator reduces the volume of oil and improves the dynamic properties of the HSA. When the control valve must operate, a positive or negative 0-10 V command signal is used. A positive voltage will shift the spool into the “A” position, and a negative voltage will shift the spool into the “B” position. The amplifier alters the current generated in the coil by a value proportional to the command voltage, and the current developed in the coil generates a magnetic field that shifts the valve spool.

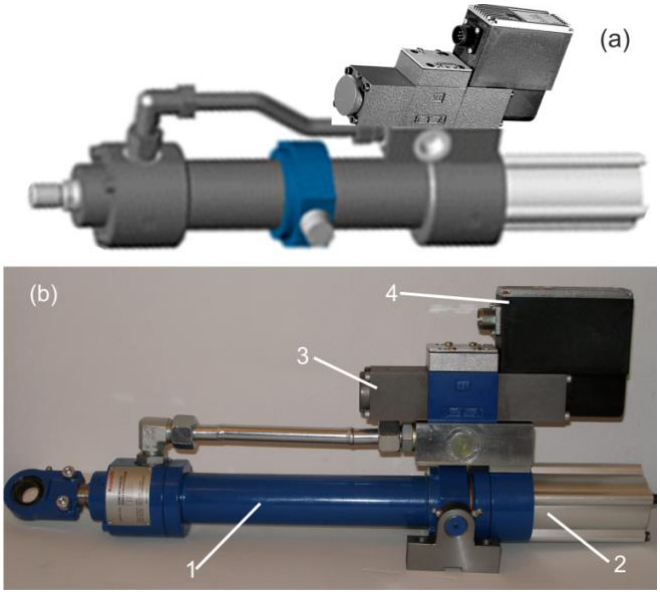

Figure 4. Hydraulic servo actuator (HSA): (a) 3D model, (b) real view: 1 – hydraulic actuator, 2 – position transducer, 3 – proportional directional control valve, 4 – integrated electronics (OBE)

Hydraulic actuator parameters: piston diameter $D = 0.05$ m, piston rod diameter $d = 0.028$ m, area ratio $\alpha = 0.69$, stroke $h = 1250$ m, stroke velocity v = 0.1 ms^{-1} for flow rate, working pressure $p = 24$ MPa. Technical data of the 4WRSE valve: nominal volumetric flow rate $q_{vn} = 35$ L/min (0.583 10^{-3} m^{3}s^{-1}) at 1 MPa pressure differential, power supply 24VDC, command value $u = \pm 10$ V, mineral oils HLP46 (kinematic viscosity $v = 0.46$ 10^{-4}m^{2}s^{-1} at temperature $T = 313.15$ K). The hydraulic actuator contains the internal magnetostrictive linear-position transducer. Therefore, the HSA is a closed-loop position control system.

The first stage of the study was to determine the dynamic model and perform a simulation of an HSA when the cylinder is rigidly mounted to the main boom and the piston rod end is flexibly connected to the internal boom through an SDD. Figure 5 shows a computational model of an HSA flexibly connected to the load mass via an SDD.

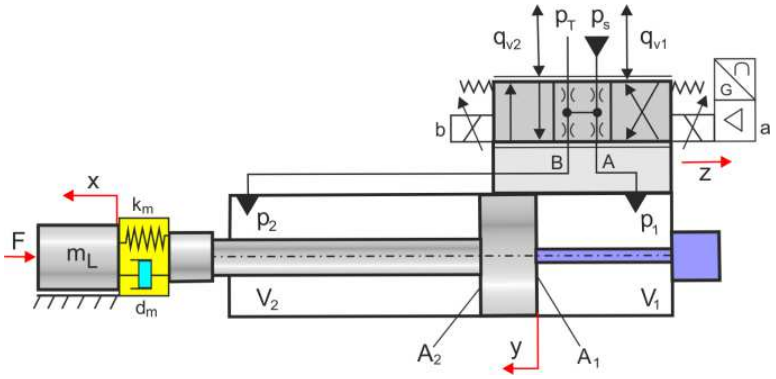

Figure 5. A computational model of an HSA flexibly connected to the load mass through an SDD

The following state coordinates were assumed in the HSA dynamic model:

– displacement x, velocity $v_x = dx/dt$, and acceleration $a_x = d^2x/dt^2$ of the mass load,

– displacement y, velocity $v_y = dy/dt$, and acceleration $a_y = d^2y/dt^2$ of the actuator piston,

– shift z and velocity $v_z = dz/dt$ of the control valve spool (the spool shift z is related to the command signal u by first-order PT1 system),

– pressure p and pressure impulse (pressure time derivative) $p_i = dp/dt$ in the actuator chambers.

Since a dynamic system with two degrees of freedom is being considered, the coordinate differences $\Delta x = x - y$, $\Delta y = y - x$ into dynamic equations were introduced. Finally, the dynamic model of IEHA flexibly connected to mass load was written as follows

$$\begin{cases} \ddot{x} = \dfrac{1}{m_L}\left[-d_m\,\Delta\dot{x} - k_m\,\Delta x - F_C + F(t)\right] \\ \ddot{y} = \dfrac{1}{m_y}\left[-d_m\,\Delta\dot{y} - k_m\,\Delta y - F_f + F_L\right] \\ \dot{z} = -\dfrac{1}{T_z}\,z + \dfrac{K_z}{T_z}\,u \\ \dot{p}_1 = \dfrac{1}{C_1}\left[q_{v1} - A_1\,\Delta\dot{y} - k_l\left(p_1 - p_2\right)\right] \\ \dot{p}_2 = \dfrac{1}{C_2}\left[-q_{v2} + A_2\,\Delta\dot{y} + k_l\left(p_1 - p_2\right) - k_{le}\,p_2\right] \end{cases} \tag{1}$$

where m_L is the load mass, d_m is the damping *coefficients*, k_m is the spring stiffness *coefficients*, F_C is the Coulomb friction force, m_y is the moving-mass of the actuator, A_1 and A_2 are the effective areas of actuator's piston, k_l is the coefficient of internal leakage flow, k_{le} is the coefficient of external leakage flow, T_z is the time constant and K_z is the gain factor of the proportional control valve dynamic [19],

$F(t)$ is the excitation force limited to harmonic vibration

$$F(t) = F_0 + F_A \sin\left(2\pi f_e t\right) \tag{2}$$

where F_0 is the constant component of the force, F_A is the excitation force amplitude, and f_e is the excitation frequency,

F_L is the load force of the hydraulic actuator

$$F_L = A_1\,p_1 - A_2\,p_2 = A_1\left(p_1 - \alpha\,p_2\right) = A_1\,p_L \tag{3}$$

where α is the area ratio, $\alpha = A_1/A_2$, and p_L is the load pressure

$$p_L = \frac{F_L}{A_1} = p_1 - \alpha\,p_2 \tag{4}$$

F_f is the friction force a function of piston velocity

$$F_f = d_y\,\dot{y} + F_{st}\exp^{-\sigma|\dot{y}(t)|}\,sign\left(\dot{y}(t)\right) + F_S \tag{5}$$

where d_y is the viscous friction coefficient, F_{st} is the static friction force, and σ is the variable coefficient.

The total friction force F_S in the seals of the hydraulic actuator is the sum of the friction force F_C due to seal squeeze and the friction force F_H due to hydraulic pressure on the seal [20]

$$F_S = F_C + F_H = f_C\,L + f_H\,A \tag{6}$$

where f_C is the friction force per seal contact length, L is the circumference for piston groove seal, $L = \pi D_o$, D_o – is the piston groove outer diameter, f_H is the friction force per projected area of seal, A is the projected area of seal for piston groove, $A = \pi/4 (D_{o2}\text{-}d_{i2})$, and d_i is the piston groove inner diameter,

C_1 and C_2 are the hydraulic capacities in the actuator chambers for the $y_0 = 0$ initial position of the actuator piston,

$$C_1 = \frac{V_1}{K} = \frac{V_{10} + A_1 \Delta y}{K} \tag{7}$$

$$C_2 = \frac{V_2}{K} = \frac{V_{20} + A_2 (h - \Delta y)}{K} \tag{8}$$

where K is the bulk modulus, V_{10} and V_{20} are the dead volumes of the cylinder chamber, and h is the stroke of actuator piston,

q_v is the symmetric flow rate through the 4/3 directional proportional control valve (A+A type, underlap)

$$q_{v1} = K_q (z_o + z) \sqrt{|\Delta p_1|}\ sign(\Delta p_1) \tag{9}$$

$$\Delta p_1 = \begin{cases} p_0 - p_1, & y \geq 0 \\ p_1 - p_T, & y < 0 \end{cases} \tag{10}$$

$$q_{v2} = K_q (z_0 - z) \sqrt{|\Delta p_2|}\ sign(\Delta p_2) \tag{11}$$

$$\Delta p_2 = \begin{cases} p_0 - p_2, & y < 0 \\ p_2 - p_T, & y \geq 0 \end{cases} \tag{12}$$

where p_0 is the supply pressure, p_T is the pressure in the tank, z_0 is the underlap valve spool, and K_q is the flow gain coefficient of the control valve

$$K_q = \frac{q_{vn}}{z_n \sqrt{\Delta p_n}} \tag{13}$$

where q_{vn} is the nominal flow rate at the pressure drop $\Delta p_n = 1$MPa and z_n is the nominal shift of the valve spool.

The formulas for the pressures in the cylinder chambers in the initial state of valve flow rate: P→A: q_v, B→T: $q_v/2$, P→B: q_v, A →T: $q_v/2$, were determined [21]

$$p_{10} = \frac{\alpha^3 p_0 + p_L}{1 + \alpha^3} \qquad p_{20} = \frac{\alpha^2 (p_0 - p_L)}{1 + \alpha^3} \tag{14}$$

where p_0 is the supply pressure.

4. Simulation results

The purpose of simulation tests is to assess the dynamic properties of a hydraulic servo actuator (HSA) rigidly and flexibly connected to a load mass. In the case of the analysed manipulator with a telescopic boom, it will be interesting to compare the step response for a rigid and flexible connection of an actuator piston rod with a load mass at a constant force and cyclic force.

Constant parameter values have been introduced into the simulation model: p_0 = 24MPa, m_y = 5kg, d_y = 2500 Ns/m, α = 0.68, A_1 = 1.96 10_{-3} m_2, A_2 = 1.3 10_{-3} m_2, V_{10} = 0.1 10_{-3} m_3, V_{20} = 0.1 10_{-3} m_3, H = 1.2 m, C_d = 0.56, d_z = 6 10_{-3} m, z_0 = 2.16x10_{-3} m, T_z = 0.01 s, ρ = 900 kg, K = 1800 MPa for ISO32 mineral oil, F_C = 500 N, F_{st} =200 N, m_L = 250 kg, F_0 = 2500 N.

Whereas, variable parameter values of SDD were adopted from the ranges: d_m = 10,000-25,000 Ns/m, k_m = 1 10_4 – 10 10_4 N/m. The initial coordinate values are as follows: x = 0, v_x= 0, y = 0; v_y= 0, z = 0, v_z= 0.

The actuator vibrations are excited by a cyclic load at the piston rod end (e.g. impact excitation). To compare the results of simulation tests, the frequency ratios of the hydraulic system, the mechanical system, and the excitation system were introduced.

Rigidly connected load mass

Hydraulic oil in an actuator chamber is compressible and thus acts like a very stiff spring. The spring stiffness k_y of the asymmetric actuator resulting from the oil stiffnesses in the cylinder chambers connected in series is

$$k_y = \left(\frac{A_1^2}{C_1} + \frac{A_2^2}{C_2} \right) = K \left(\frac{A_1^2}{V_1} + \frac{A_2^2}{V_2} \right) \tag{15}$$

The natural frequency f_y of the actuator excited by the cyclic load is

$$f_y = \frac{1}{2\pi} \sqrt{\frac{k_y}{m_y + m_L}} \tag{16}$$

The excitation frequency f_e results from the rock breaker frequency

$$f_e = \frac{f_{rb}}{60} \tag{17}$$

where f_{rb} is the rock breaker frequency in bpm (beats per minute).

The frequency ratio fr for a rigid connection is as follows

$$fr = \frac{f_e}{f_y} \tag{18}$$

Figure 6 shows the natural frequency f_y of the asymmetrical hydraulic actuator versus piston displacement y over the stroke length h. Therefore, the relative frequency fr was defined as the ratio of the excitation frequency f_e to the natural frequency f_y of a hydraulic actuator. The relative frequency f_r versus piston displacement y for the asymmetrical hydraulic actuator exciting by the cyclic load is shown in Figure 7. Such a rock breaker was selected to avoid resonant vibrations when the exciting frequency f_e is close to the natural frequency f_y of the actuator ($fr \approx 1$).

As can be seen from Figure 6, the lowest value the natural frequency of a hydraulic actuator is $f_y \approx 30$Hz. From this it follows that the hydraulic actuator is suitable for machines requiring high dynamics [22].

The dynamic properties of the servo hydraulic actuator depend on the ratio of the frequency f_y of the actuator to the frequency f_z of the control valve

$$fd = \frac{f_y}{f_z} \tag{19}$$

The value of fd is a tip for selecting an HSA controller; in the analysed case fd = 0.3-1.

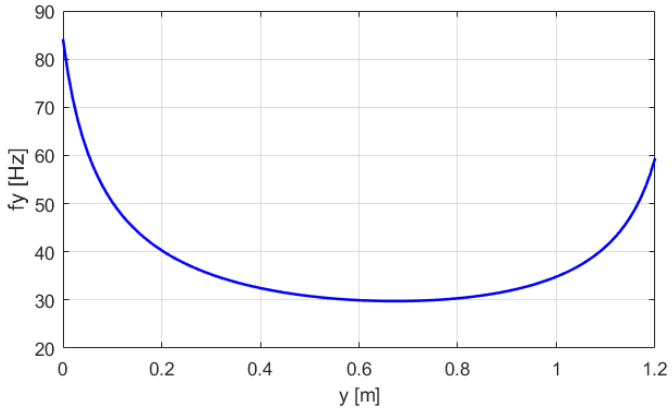

Figure 6. Natural frequency f_y of the asymmetrical hydraulic actuator versus piston displacement y over the stroke length h

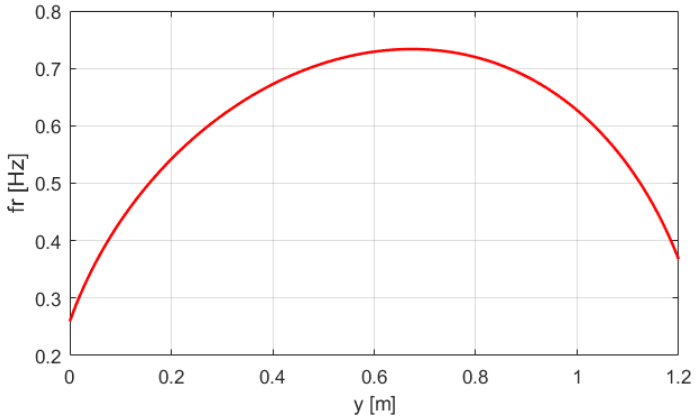

Figure 7. Relative frequency f_r versus piston displacement y for the asymmetrical hydraulic actuator exciting by the cyclic load

The dynamic responses of the displacements $y(t)$ and the speeds $v_y(t)$ of of an HSA rigidly connected to a load mass m_L = 250kg for y_{set} = 0.6m, a constant force F_0 = 2500N (blue line), and excitation force $F(t)$ (red line) at frequency f_e = 21.8Hz are compared in Figure 8.

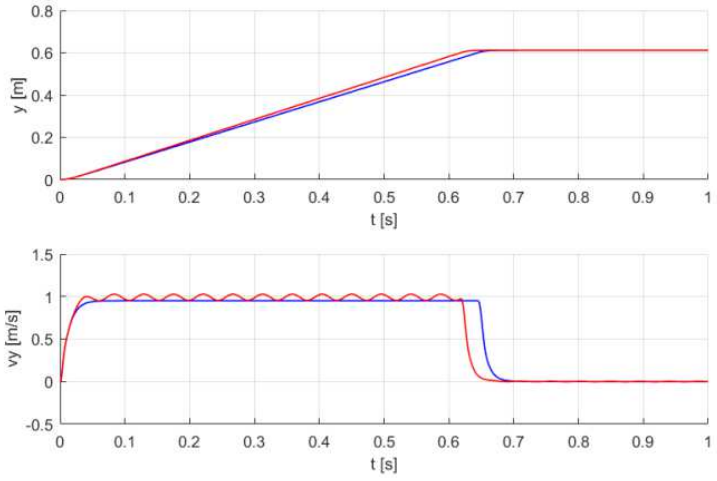

Figure 8. Comparison of dynamic responses of the displacements $y(t)$ and the speeds $v_y(t)$ of an HSA rigidly connected to a load mass

The dynamic responses of the load pressures $p_L(t)$ in an HSA rigidly connected to a load mass $m_L = 250$kg for $y_{set} = 0.6$m, a constant force $F_0 = 2500$N (blue line), and excitation force $F(t)$ (red line) at frequency $f_E = 21.8$Hz are compared in Figure 9.

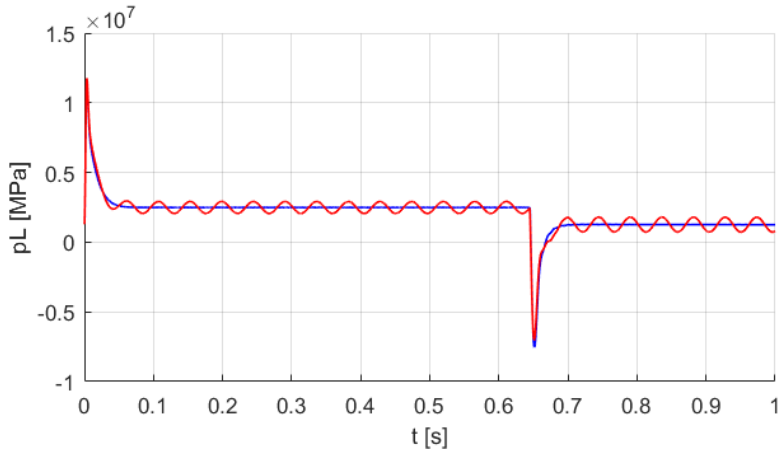

Figure 9. Comparison of dynamic responses of the load pressures $p_L(t)$ in an HSA rigidly connected to a load mass

The piston stroke setting y_{set} of the hydraulic actuator in which the control valve ports are blocked is taken into account. For this stroke, the equations of the piston motion and the equations of flow continuity in the chambers of the actuator excited by cyclic force were written

$$\begin{cases} \ddot{y} = \dfrac{1}{m_y + m_L}\left[-d_y\ \dot{y} - \left(A_1\ p_1 - A_2\ p_2\right) + F(t)\right] \\ \dot{p}_1 = \dfrac{1}{C_{1set}}\ A_1\ \dot{y} \\ \dot{p}_2 = -\dfrac{1}{C_{2set}}\ A_2\ \dot{y} \end{cases} \tag{20}$$

where C_{1set} and C_{2aet} are the hydraulic capacities in the actuator chambers for y_{set}

$$C_{1set} = \frac{V_{1s}}{K} = \frac{V_{10} + A_1\ y_{set}}{K} \tag{21}$$

$$C_{2set} = \frac{V_{2s}}{K} = \frac{V_{20} + A_2\left(h - y_{set}\right)}{K} \tag{22}$$

For the analysed piston stroke setting y_{set}, The displacement $y(t)$ and the speed $v_y(t)$ of an actuator rigidly connected to a load mass $m_L = 250$kg for $y_{set} = 0.6$m and excitation force $F(t)$ at frequency $f_e = 21.8$Hz are shown in Figure 10.

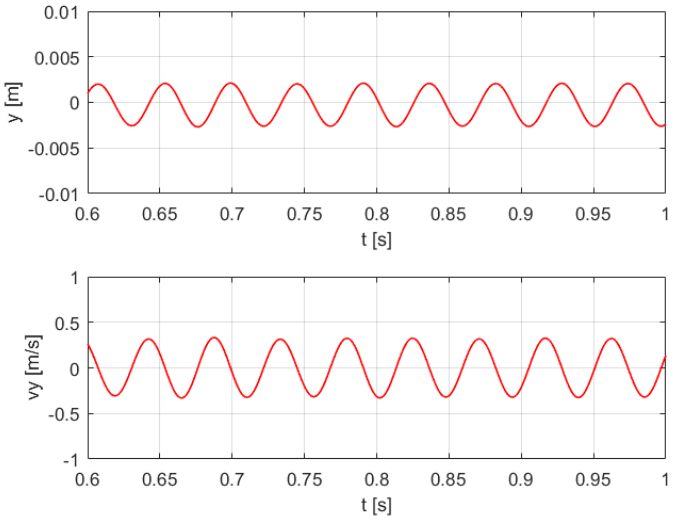

Figure 10. The displacement $y(t)$ and the speed $v_y(t)$ of an actuator rigidly connected to a load mass

For such a piston stroke setting, the pulsation of pressures $p_1(t)$ and $p_2(t)$ in an actuator rigidly connected to a load mass m_L = 250kg for y_{set} = 0.6m and excitation force $F(t)$ at frequency f_E = 21.8Hz are shown in Figure 11.

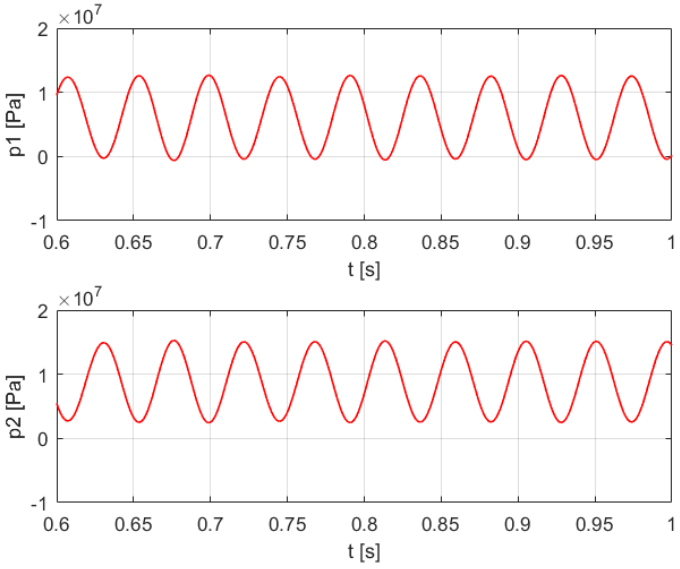

Figure 11. Pulsation of pressures $p_1(t)$ and $p_2(t)$ in an actuator rigidly connected to a load mass

Flexibly connected load mass

The natural frequency f_y of the actuator:

$$f_y = \frac{1}{2\pi}\sqrt{\frac{k_y}{m_y}} \tag{23}$$

The natural frequency f_m of the mechanical components of the SDD

$$f_m = \frac{1}{2\pi}\sqrt{\frac{k_m}{m_L}} \tag{24}$$

The frequency ratios fr_{ym} and fr_{em} for a flexible connection are as follows

$$fr_{ym} = \frac{f_y}{f_m} \tag{25}$$

$$fr_{em} = \frac{f_e}{f_m} \tag{26}$$

The damping ratio ξ_y of the actuator

$$\xi_y = \frac{d_y}{2\sqrt{k_y m_y}} \tag{27}$$

The damping ratio ξ_m of mechanical components of the SDD

$$\xi_m = \frac{d_m}{2\sqrt{k_m m_L}} \tag{28}$$

The relative damping rd_{my} for a flexible connection is as follows

$$rd_{my} = \frac{\xi_m}{\xi_y} = \frac{d_m}{d_y}\sqrt{\frac{k_y}{k_m}}\sqrt{\frac{m_y}{m_L}} \tag{29}$$

For the analysed setting y_{set} the frequency ratios are $fr_{ym} = 95.01$, $fr_{em} = 9.7$, and the relative damping is $rd_{my} = 11.4$.

Figure 12 compares the dynamic responses of the displacements $x(t)$ and speeds $v_x(t)$ of a mechanical system at load mass $m_L = 250$kg for $y_{set} = 0.6$m, a constant force $F_0 = 2500$N (blue line) and excitation force $F(t)$ (red line) at frequency $f_e = 21.8$Hz

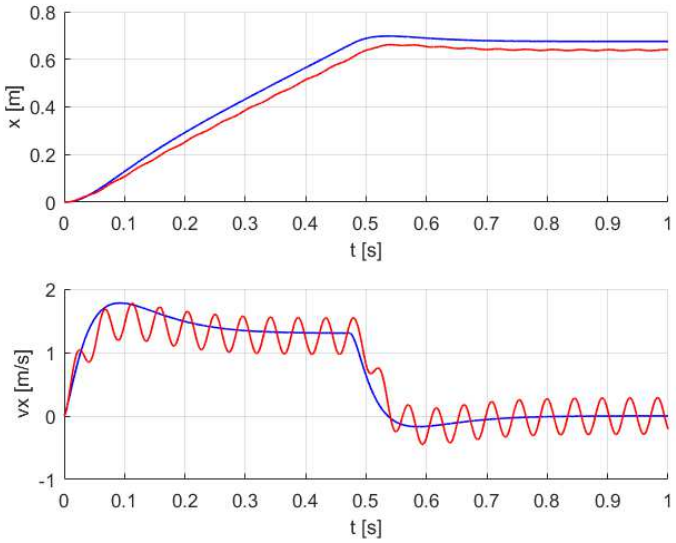

Figure 12. Comparison of dynamic responses of a mechanical system consisting of a load mass and an SDD

The dynamic responses of the displacement $y(t)$ and speed $v_y(t)$ of an HSA flexibly connected to a load mass $m_L = 250$kg for $y_{set} = 0.6$m, constant force $F_0 = 2500$N (blue line) and excitation force $F(t)$ (red line) at frequency $f_e = 21.8$Hz are compared in Figure 13.

The dynamic responses of the load pressures $p_L(t)$ in an HSA flexibly connected to a load mass $m_L = 250$kg for $y_{set} = 0.6$m, a constant force $F_0 = 2500$N (blue line), and excitation force $F(t)$ (red line) at frequency $fe = 21.8$Hz are compared in Figure 14.

The dynamic responses of the load pressures $p_L(t)$ of an HSA flexibly connected to a load mass for a constant load force and an excitation force

The dynamic responses of the displacements $y(t)$ and the speeds $v_y(t)$ of an HSA rigidly (green line) and flexibly (red line) connected to a load mass $m_L = 250$kg for $y_{set} = 0.6$m and excitation force $F(t)$ at frequency $f_e = 21.8$Hzare compared in Figure 15.

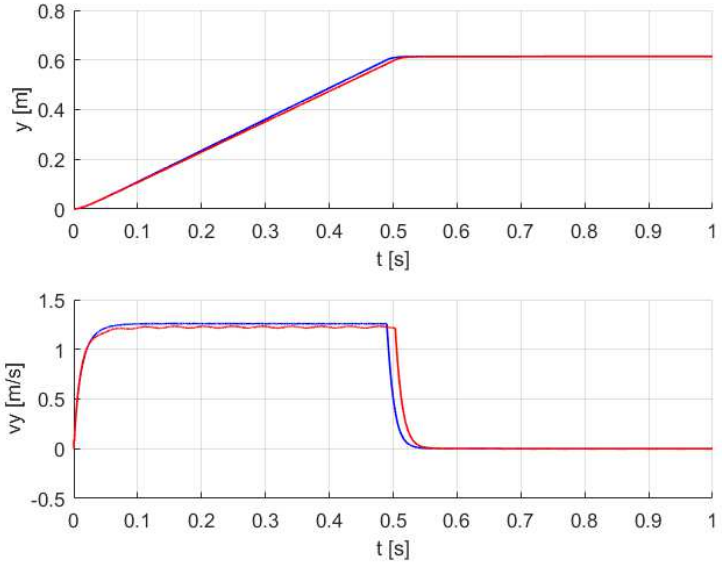

Figure 13. Comparison of dynamic responses of the displacement $y(t)$ and speed $v_y(t)$ of an HSA flexibly connected to a load mass

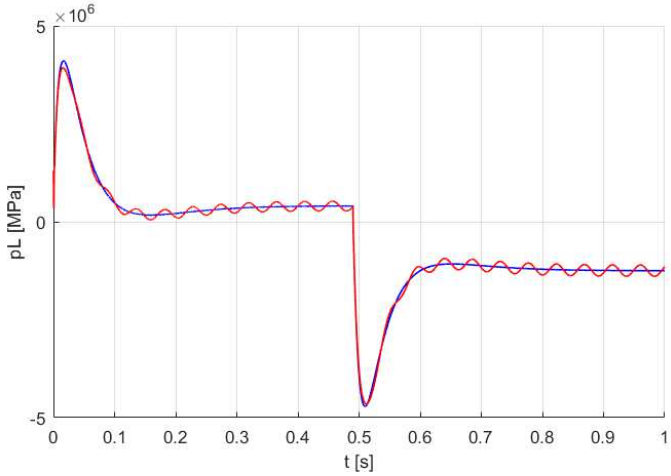

Figure 14. Comparison of dynamic responses of the load pressures $p_L(t)$ in an HSA flexibly connected to a load mass

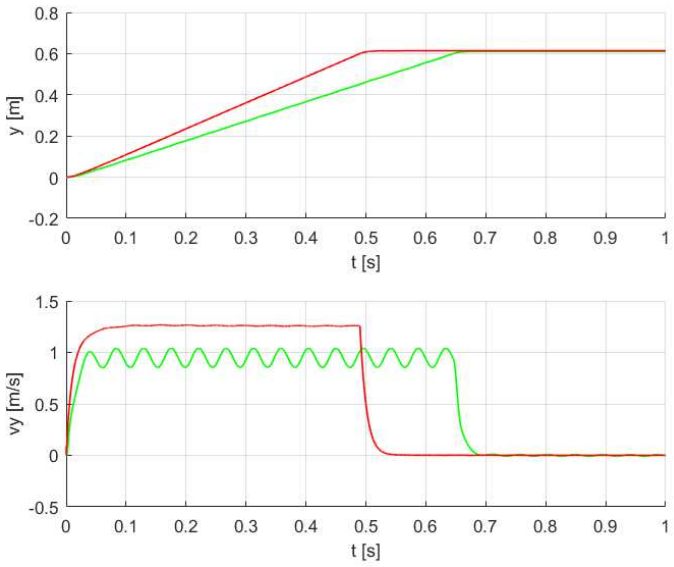

Figure 15. Comparison of dynamic responses of the displacements $y(t)$ and the speeds $v_y(t)$ of an HSA rigidly (green line) and flexibly (red line) connected to a load mass

The dynamic responses of the load pressures $p_L(t)$ in a hydraulic actuator rigidly (green line) and flexibly (red line) connected to a load mass m_L = 250kg for y_{set} = 0.6m and excitation force $F(t)$ at frequency f_e = 21.8Hz are compared in Figure 16.

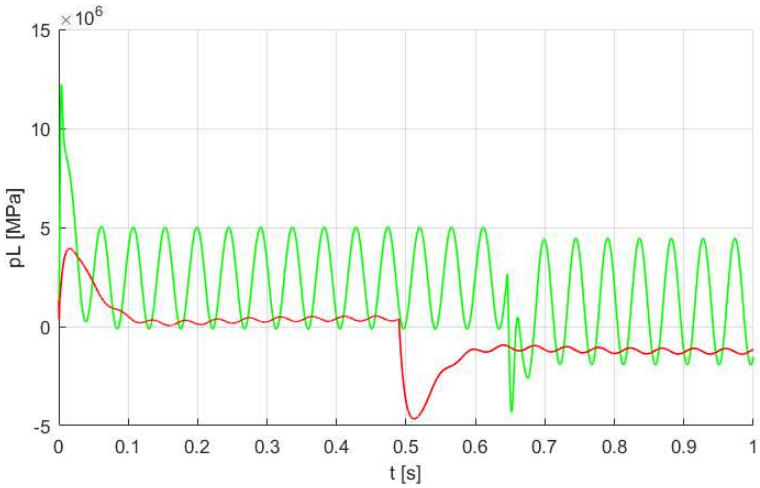

Figure 16. Comparison of dynamic responses of the load pressures $p_L(t)$ in a hydraulic actuator rigidly (green line) and flexibly (red line) connected to a load mass

Based on the simulation tests of an HSA flexibly connected to a load mass, various parametric relationships were compared. When designing HSA with a flexible combined mass load, an experimental analysis is needed to confirm the theoretical assumptions.

5. Experimental results

The purpose of the experimental test is to choose such a control algorithm for a hydraulic servo actuator (HSA) with flexibly connected load mass that will ensure the extension and retraction of the internal telescopic boom without vibration interference. The view of the test stand of the HSA is shown in Figure 17. A mass load of the hydraulic actuator as the technological payload is achieved by weights installed on the linear guide support. To

generate a constant force on the working actuator, a loading hydraulic actuator was used. An electro-hydraulic vibration exciter with two rotary valves to generate the excitation force was used. The displacement of the linear hydraulic actuator (CSM1/MT4/50/28/1200) is measured using the m*agnetostrictive linear-position sensor (*Novostrictive® TMI 0250 with CANopen interface*)*. The 4/3 proportional directional valve (4WRSE6V1-35-3X/G24K0/A1) is used for position and speed control of the hydraulic actuator. In the test stand, the technological load is measured using a force sensor. The supply pressure (p_{max} = 24 MPa) is set by a proportional pressure relive valve (DBETX–1X/250G24–25NZ4M). The test stand also includes a computer system in the superior control system equipped with the Matlab/Simulink (xPC Target) software. The PC has C/A and A/C converter cards of PCI type DAS1602/16 Measurement Computing Corporation. The card, along with the actuator position converter, creates the measurement system. In the experimental test, the measuring signals were taken from sensors as continuous signals, and then after the discretisation of signals registered digitally.

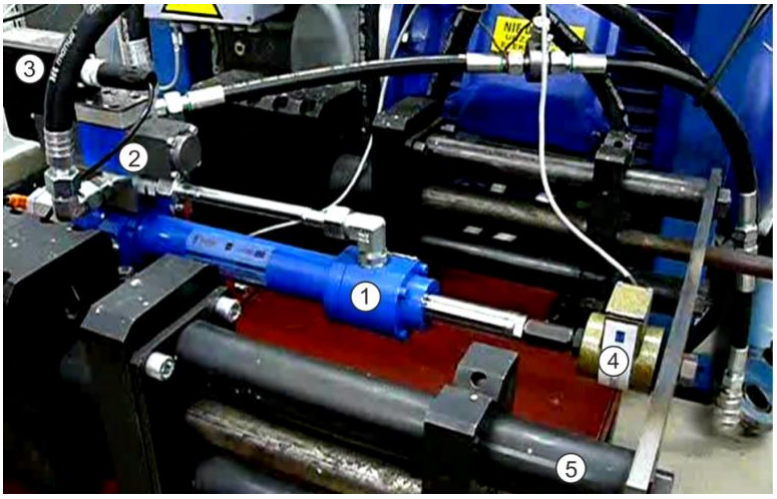

Figure 17. Experimental test-stand: 1 – hydraulic actuator, 2 – proportional control valve, 3 – integrated electronics (OBE), 4 – spring-damping device (SDD), 5 – slider with the mass load

The position control system of an HSA using an indirect adaptive control method is shown in Figure 18.

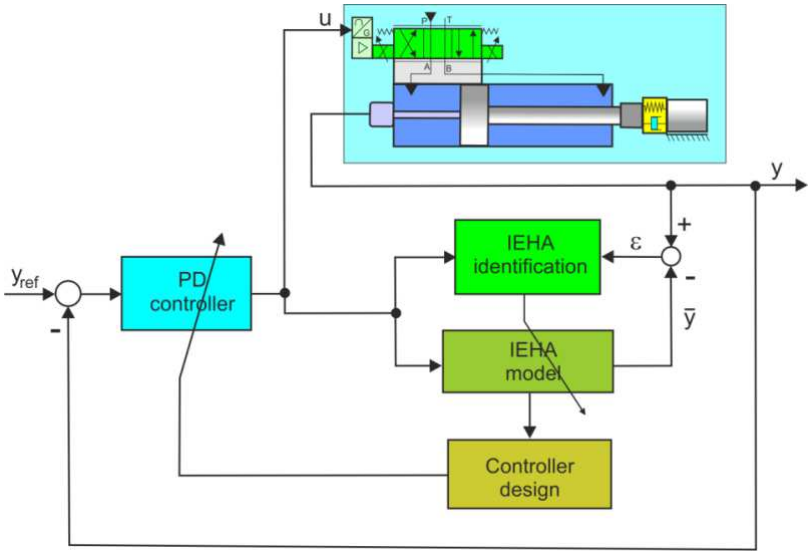

Figure 18. Test stand diagram of the position adaptive control system of an HSA flexibly connected to mass load

The main task was to adapt the adaptive position controller to the identified HSA loaded with excitation force (impact force). From an ordinary system with feedback, the adaptive system used distinguishes information in the form of a defined reference model. The equivalent G_0 discrete transfer function of an HSA as a controlled object was given by [23]

$$\frac{y_k}{u_k} = G_0(z^{-1}) = \frac{z^{-d}B(z^{-1})}{A(z^{-1})} \tag{30}$$

where: y_k is the output signals in discrete time, u_k is the control signals in discrete time, z is the backward shift (delay) operator, d is the discreet delay determined by the number of sampling periods, and $A(z^{-1})$ and $B(z^{-1})$ are the polynomials in z^{-1} for zero initial conditions, and z-transform is the backward shift (unit delay) operator. That is

$$\begin{cases} A(z^{-1}) = 1 + a_1 z^{-1} + a_2 z^{-2} + \cdots + a_m z^{-m} \\ B(z^{-1}) = b_1 z^{-1} + b_2 z^{-2} + \cdots + b_n z^{-n} \end{cases} \tag{31}$$

where a_1, a_2,...,a_n are the feedback coefficients, b_1, b_2,...,b_n are the feedforward coefficients, n and m are the degrees of polynomials.

Figure 19 shows the PD controller tuning method.

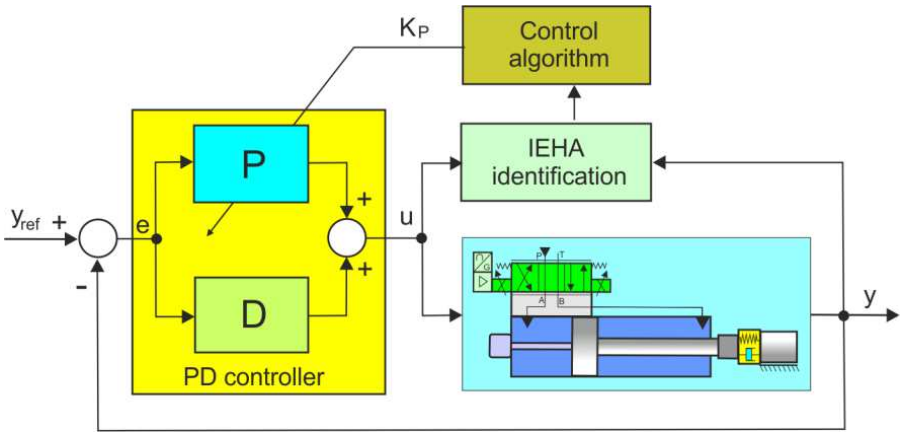

Figure 19. Tuning the PD controller: P – proportional controller, D – derivative controller, y_{ref} – input (reference) signal, e – error signal, u – control (actuating) signal, y – output signal

The discrete-time PD (proportional-derivative) controller was selected for HSA position control

$$u_k = K_P\left[e_k + \frac{T_D}{T_p}(e_k - e_{k-1})\right] = K_P e_k\left[1 + \frac{T_D}{T_p}\left(1 - \frac{e_{k-1}}{e_k}\right)\right] \tag{32}$$

where K_P is the proportional gain, T_D is the derivative time, T_p is the sampling time, e_k is the error signal, $e_k = y_{kref} - y_k$, y_{kref} is the input (reference) signal, y_k is the output signal.

If the PD controller depends only on gain factor K_P, then the transfer function is

$$\frac{u_k}{e_k} = G_P(z^{-1}) = K_P \tag{33}$$

In the IEHA control system, the expression of closed-loop transfer function G_z was adopted in the form

$$\frac{y_k}{y_{kref}} = G_z(z^{-1}) = \frac{G_P(z^{-1})\ G_0(z^{-1})}{1 + G_P(z^{-1})\ G_0(z^{-1})} \tag{34}$$

After substituting (30) and (33) to (34), the discrete transfer function G_z is represented in the form

$$G_z(z^{-1}) = \frac{z^{-d} K_P B(z^{-1})}{A(z^{-1}) + z^{-d} K_P B(z^{-1})} \tag{35}$$

The denominator D(z) of the transfer function (35) is used to determine stable poles

$$D(z^{-1}) = A(z^{-1}) + z^{-d} K_P B(z^{-1}) \tag{36}$$

The optimum setting of the PD controller depends on gain factor $K_P = K_{Pcr}(T_{pcr})$, where K_{Pcr} is the critical proportional gain, and T_{pcr} is the critical period of oscillation set at the limit of controller stability (the controller tuning process occurs in real-time throughout the life of the system). The task is to select the gain factor $K_P = K_{Pcr}(T_{pcr})$ so that the control closed system was stable, which means that the characteristic equation (35) has z_i roots which comply with the conditions $z_i < 1$ for $i = 1,2,..,m$. Figure 20 shows tuning parameters K_{pcr} and T_{crr} of the PD controller for HSA positioning control.

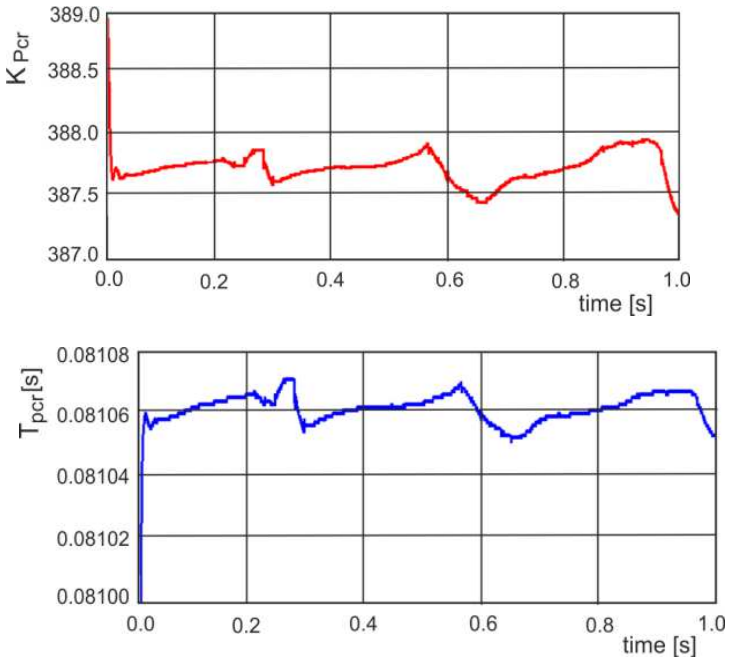

Figure 20. Tuning parameters K_{Pcr} and T_{pcr} of the PD controller

Figure 21 shows the courses of the desired and measured forces $F(t)$ at excitation frequency 21.8 Hz.

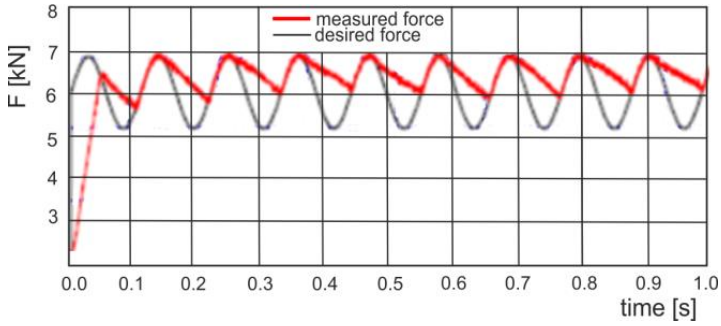

Figure 21. Desired and measured excitation force $F(t)$

Figure 22 presents the experimental results of displacement $y(t)$ and position error ε_y of an HSA rigidly connected to a load mass for references position y_{ref} = 0.6 m and excitation force at frequency 21.8 Hz.

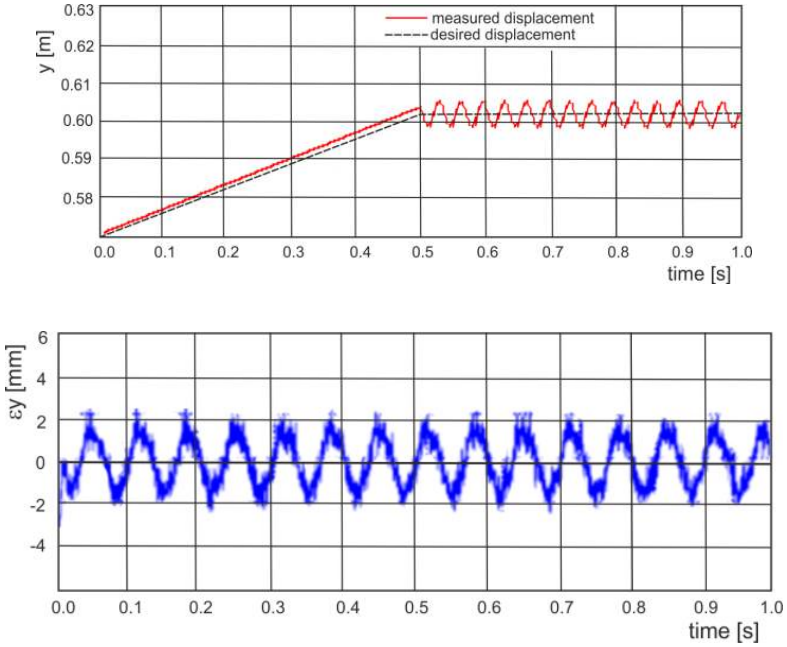

Figure 22. Experimental results of the displacement y(t) and positioning error $\varepsilon_y(t)$ of an HSA rigidly connected to a load mass

Dynamic characteristics in the steady-state range for a hydraulic cylinder rigidly and flexibly connected to a load mass in the case of excitation force at frequency f_e = 21.8Hz are shown in Figure 23.

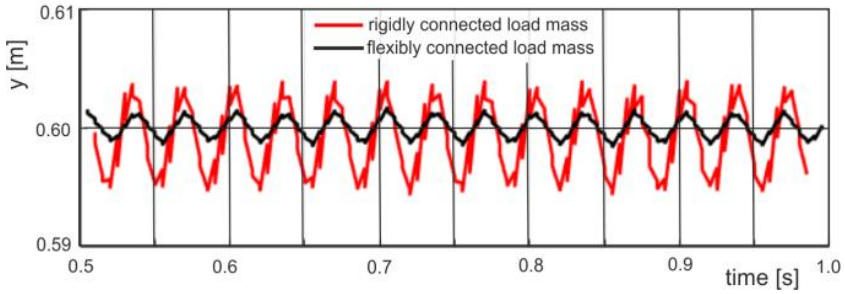

Figure 23. Comparisons of the dynamic characteristics in the steady-state range for a hydraulic actuator rigidly and flexibly connected to the load mass in the case of excitation force

6. Conclusions

The study deals with a hydraulic servo actuator (HSA) flexibly connected to a load mass via spring-damping devices (SDD). In this case, an SDD was used for vibration isolation of cyclic forces exciting by a rock breaker. The interaction of cyclic forces on the dynamics and control of an HSA is a rather complex dynamic problem that is completely overlooked by researchers and designers of hydraulic drives. HSA tests with vibration loading are of particular importance for large-scale heavy-duty hydraulic equipment used in construction equipment, mining machines, etc., in which there are large moving masses and where design may have a mechanical compliant structure. The special case of using an HSA in a newly designed 3-DoF hydraulic boom manipulator to move a medium-sized hydraulic rock breaker was analysed. The manipulator attached to the jaw crusher has a working area that allows for the crushing of rock that are too large on the rock conveyor or in the crusher's feed gape.

A particular dynamic task was considered in which an HSA was rigidly mounted to the mother boom and where the piston rod was flexibly connected via an SDD to the inner boom of a hydraulic manipulator. Simulation tests based on the HSA mathematical model enabled comparison of the dynamic responses of a hydraulic actuator rigidly connected and flexibly connected via an SDD to the load mass with a constant force or impact force excited by the rock breaker. The experimental studies on the test stand focused on HSA adaptive positioning control. The main task was to adapt the adaptive position controller to the identified HSA loaded with excitation force (impact force). A rock breaker was chosen so that its natural frequency was higher than the resonance frequency of the HSA.

The studies carried out are of great importance for assessing dynamic properties and designing a controller for position control of an HSA subjected to cyclic impact forces. The presented results are also important for the development of guidelines for the safe operation of various large-scale heavy hydraulic machines under vibration loads. All the results presented in this article are original, as there were no similar studies before. There is no publicly available data from other authors on the studies presented in this work. The limitations of the study findings are related to the parameters of the designed 3-Dof hydraulic boom manipulator and the selected rock breaker. The HSA and SDD were adapted to these restrictions. This restriction also implies an impact force at a frequency limited to 21.8Hz. Further research should include a reliability analysis of hydraulic actuators loaded with large moving masses and vibration forces.

The most important conclusions resulting from conducting the study are as follows:

1. If, during the design phase, flexible connections of the hydraulic actuator are omitted, they may become a "parasitic" load, which will contribute to the deterioration of the dynamic properties of the HSA.
2. The conducted tests proved that it is justified to introduce a mechanical vibration isolator into a hydraulic actuator excited by cyclic forces.
3. After including an additional mechanical mass-damper-spring system, the degree of differential equations of the modelled dynamic system increases, which complicates its responses characteristics and their assessment.
4. Taking into account the cyclic loads of a certain frequency implies a frequency analysis of the dynamics system.
5. The operation of an HSA in the near range of resonance frequencies is practically unacceptable, as this leads to unstable and uninhibited control.

6. The introduction of an SDD improves the dynamic properties of an has, because the hydraulic actuator has low damping.

7. Declarations:

Availability of data and materials:

- The datasets used and/or analysed during the current study are available from the corresponding author on reasonable request.
- Selected data generated or analysed during this study are included in this published article.

Competing interests: The authors declare that they have no competing interests.

Funding: Not applicable.

Author Contributions: Conceptualization, methodology, software, formal analysis, resources, writing—original draft preparation, writing—review, and editing, visualization, supervision R.D.; data curation, investigation, validation P.W.;All authors have read and agreed to the published version of the manuscript.

Acknowledgements: Not applicable.

Authors' information:

Ryszard Dindorf is a Professor of the Department of Manufacturing Engineering and Metrology at Faculty of Mechatronics and Mechanical Engineering of Kielce University of Technology (Poland). His research activities include fluid power control and mechatronic systems - hydraulic and pneumatic drives in the automation and robotization of production processes. He was a member of Committee on Automatic Control and Robotics of Polish Academy of Sciences.

Piotr Wos is a post doctor of the Department of Manufacturing Engineering and Metrology at Faculty of Mechatronics and Mechanical Engineering of Kielce University of Technology (Poland), where he is currently a lecturer. His main research interests are in adaptive control and real-time control systems. He is focused on applications for hydraulic and pneumatic drives and sensory systems.

References

1. Jelali, M., Kroll, A. (2003). Hydraulic servo-systems. Modelling, identification and control. Springer, London.
2. Helduser, S. (1977). Einfluss der Elastizität mechanischer Übertragungselemente auf das dynamische Verhalten hydraulischer Servoantriebe. *Dissertation*, TU Aachen, Aachen.
3. Cetinkunt, S. (2015) Mechatronics with experiment. Wiley, New Delhi.
4. Walters, R.B. (1991). Hydraulic and electro-hydraulic control systems. Elsevier Applied Science, London, New York.
5. Feng, H., Du, Q., Huang, Y., Chi, Y. (2017). Modelling study on stiffness characteristics of the hydraulic cylinder under multi-factors. *Journal of Mechanical Engineering,* **63**(7-8): 447-456. DOI: https://doi.org/10.5545/sv-jme.2017.4313

6. Tang, H., Ren, V. (2015). Research on rigid-flexible coupling dynamic characteristics of a boom system in a concrete pump truck. *Advances in Mechanical Engineering,* **7**(2), 1–7. DOI: https://doi.org/10.1177/1687814015573854
7. Sochacki, W., Tomski, L. (1999). Free vibration and dynamic stability of hydraulic cylinder set. *Machine Dynamics Problems,* **23**(4), 91-104.
8. Gürgöze, M., Doğruoğlu, S.N., Aeren, S. (2007). On the eigencharacteristics of a cantilevered visco-elastic beam carrying a tip mass and its representation by a spring-damper-mass system. *Journal of Sound and Vibration*, **301**, 420-426. DOI: https://***doi***.org/***10.1016/j.jsv.2006.10.002***
9. Taha, M.H., Abohadima, S. (2008). Mathematical model for vibrations of non-uniform flexural beams. *Engineering Mechanics,* **15**(1), 3-11.
10. Zhang, T., Zhang, N. (2016). Vibration modes and the dynamic behavior of a hydraulic plunger pump. *Shock and Vibration*, Hindawi,1-7. DOI: https://***doi***.org/10.1155/2016/9679542
11. Zhang, J., Deng, Y., Zhang, N., Zhang, B., Qi, H., Zheng, M. (2019). Vibration performance analysis of a mining vehicle with bounce and pitch tuned hydraulically interconnected suspension. *Chinese Journal of Mechanical Engineering*, **32**(5), 1-17. DOI: https://***doi***.org/***10.1186/s10033-019-0315-0***
12. Book, W.J. (1984). Recursive Lagrangian dynamics of flexible manipulator arms. *International Journal Robotics Research,* **3**, 87-101. DOI: https://doi.org/10.1177/027836498400300305
13. Bernzen, W. (1997). On vibration damping of hydraulically driven flexible robots. *Proceedings of the 5th IFAC Symposium on Robot Control,* Nantes, France, 677-682.DOI: https://doi.org/10.1016/S1474-6670(17)44330-8
14. ISO 4413:2010 Hydraulic fluid power — General rules and safety requirements for systems and their components.
15. Smith, D.J. (2001). Reliability, Maintainability and risk. Butterworth-Heinemann, Oxford.
16. Wang, S., Tomovic, M., Liu, H. (2016). Commercial Aircraft Hydraulic Systems. Academic Press Elsevier, Waltham.
17. Military standards: Hydraulic system components, ship, aircraft. U.S. (2014). Department of Defense, Washington.
18. Dindorf, R., Wos, P. (2019). Control of integrated electro-hydraulic servo-drives in a translational parallel manipulator. *Journal of Mechanical Science and Technology*, **33**(11): 5437–5448. DOI: https://***doi***.org/***10.1007/s12206-019-1038-y***
19. Dindorf, R., Wos, P. (2020). Energy-saving hot open die forging process of heavy steel forgings on an industrial hydraulic forging press. *Energies,* **13**(7), 1-17. ; DOI: **https://doi.org/10.3390/en13071620**
20. Agarwal, N.A., Lawson, C.P. (2016). Practical method to account for seal friction in aircraft hydraulic actuator preliminary design. *Proceedings of the Institution of Mechanical Engineers, Part G: Journal of Aerospace Engineering*, 231(5): 941-950. DOI: https://doi.org/10.1177/0954410016645371
21. Dindorf, R., Wos, P. (2019). Force and position control of the integrated electro-hydraulic servo-drive. *Proceedings of the 20th International Carpathian Control Conference*, Wieliczka-Krakow, Poland, 26-29 May 2019, ***IEEE Xplore 2019*****,** July, 277–282. **DOI:** 10.1109/CarpathianCC.2019.8765986
22. Design and control of proportional and servo systems. (2008). Rexroth Bosch Group AG, Erbach
23. Wos, P., Dindorf, R. (2013). Adaptive control of the electro-hydraulic servo-system with external disturbances. *Asian Journal of Control*, **15**(4), 1065–1080. **DOI:** https://doi.org/10.1002/asjc.602